OPEN ACCESS

GRS Journal of Multidisciplinary Research and Studies

Abbreviate Tittle- GRS J Mul Res Stud

ISSN *(Online) - 3049-0561*

https://grspublisher.com/journal-details/GRSJMRS

Vol-3, Iss-6 (Jun)-2026)

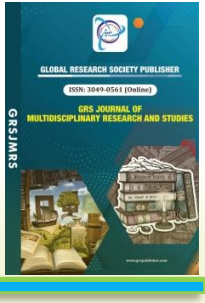

Role of Ultrasonography and Colour Doppler in Evaluation of Thyroid Nodules with Fine Needle Aspiration Cytology Correlation: A Prospective Descriptive Study

[1]Dr.Sanjay N. Totawar, [2]Dr.Satish Z. Sorte, [3]Dr.Bhawana Sonawane, [4]Dr.Anagha Deshpande

[1]Resident, Department of Radiodiagnosis, IGGMC, Nagpur – 440018

[2, 3,4]Department of Radiodiagnosis, Indira Gandhi Government Medical College & Hospital, Nagpur, Maharashtra, India – 440018.

Article History

Received: 20.05.2026

Accepted: 13.06.2026

Published: 27.06.2026

Corresponding Author: Dr.Sanjay N. Totawar

Abstract: Background & Aim: Thyroid nodules represent one of the most prevalent endocrinological findings in clinical practice, with sonographic prevalence ranging from 19–67%. The principal diagnostic challenge lies in non-invasively differentiating malignant from the far more prevalent benign thyroid nodules. This study aimed to systematically evaluate the gray scale, color Doppler flow imaging (CDFI), and spectral Doppler characteristics of thyroid nodules and to correlate these sonographic features with fine needle aspiration cytology (FNAC) findings.

Methods: This prospective, descriptive cross-sectional study was conducted at the Department of Radiodiagnosis, IGGMC, Nagpur, over a 24-month period (November 2017 – November 2019). Eighty consecutive patients presenting with thyroid swelling underwent high-resolution grayscale ultrasonography and color/spectral Doppler evaluation using a Philips HD11XE machine with a 7–12 MHz linear transducer. Nodule characteristics assessed included size, shape, echotexture, margins, halo, internal calcification, cervical lymphadenopathy, and vascularity (CDFI). Spectral Doppler parameters including peak systolic velocity (PSV), pulsatility index (PI), and resistive index (RI) were recorded. Nodules were stratified using the Thyroid Imaging Reporting and Data System (TI-RADS). All cases subsequently underwent USG-guided FNAC, and histopathological biopsy where applicable. Statistical analysis was performed using chi-square test and receiver operating characteristic (ROC) curve analysis; $p < 0.05$ was considered statistically significant.

Results: Of 80 patients (78.75% female; mean age 38.4 years), 71 (88.75%) harbored benign and 9 (11.25%) malignant nodules. Malignant lesions were significantly more frequent in patients aged >40 years ($p < 0.001$). On gray scale, irregular margins (88.89% vs 0%), hypoechogenicity (77.78% vs 8.45%), and the presence of microcalcifications (77.78% vs 42.25%) were strongly associated with malignancy (all $p < 0.05$). On CDFI, intra-nodular vascularity was present in 100% of malignant versus 19.71% of benign lesions ($p < 0.001$). Spectral Doppler demonstrated RI > 0.75 in 88.89% of malignant nodules (sensitivity 88.89%, specificity 98.59%; $p < 0.001$) and PSV ≤ 20.4 cm/s in 100% of malignant lesions ($p < 0.001$). Combined gray scale + Doppler sonography achieved an overall sensitivity of 98% and specificity of 97% for detection of thyroid malignancy. Complete concordance was achieved between USG and FNAC diagnoses for all malignant lesions. Among malignant lesions, papillary thyroid carcinoma and follicular thyroid carcinoma were the most common histotypes, each accounting for 33.33% (3/9 cases), followed by anaplastic carcinoma (22.22%) and medullary carcinoma (11.11%).

Conclusion: High-resolution gray scale ultrasonography combined with CDFI and pulse Doppler constitutes a highly sensitive, non-invasive first-line imaging modality for characterizing thyroid nodules. The combination achieves near-complete correlation with FNAC for malignant lesions, potentially reducing the need for unnecessary cytological sampling in clinically benign lesions.

***Keywords*: *Thyroid nodule; Ultrasonography; Color Doppler; Spectral Doppler; FNAC; TI-RADS; Gray scale; Malignancy; Resistive index; Peak systolic velocity*.**

Cite this Article

Dr. S. N. Totawar, Dr. S. Z. Sorte, Dr. B. Sonawane, Dr. A. Deshpande, (2026) Role of Ultrasonography and Colour Doppler in Evaluation of Thyroid Nodules with Fine Needle Aspiration Cytology Correlation: A Prospective Descriptive Study *GRS Journal of Multidisciplinary Research and Studies, Vol-3 (Iss-6). 45-58*

Introduction

Thyroid nodules are among the most common endocrine abnormalities encountered in clinical practice, with a reported sonographic prevalence of 19–67% in the general adult population. Palpation-based detection is limited to nodules ≥ 1 cm, identifying only 4–7% of all sonographically detectable lesions. In the Indian subcontinent, thyroid nodules are demonstrable in approximately 8.5% of individuals, with women disproportionately affected at a ratio of approximately 3:1.

The fundamental clinical imperative in evaluating thyroid nodules lies in reliably distinguishing the small but clinically critical

proportion of malignant lesions—estimated at 5–15%—from the majority of benign nodules, thereby appropriately stratifying patients for cytological sampling, surgical intervention, or radiological surveillance. While computed tomography (CT), magnetic resonance imaging (MRI), and radionuclide scintigraphy contribute to thyroid imaging, high-resolution ultrasonography (USG) has emerged as the pre-eminent first-line modality owing to its superior spatial resolution, real-time acquisition, absence of ionizing radiation, widespread availability, and cost-effectiveness.

Gray scale sonography provides detailed morphological characterization of thyroid nodules including size, shape, margins, internal architecture, echogenicity, calcification pattern, and halo characteristics. The introduction of the Thyroid Imaging Reporting and Data System (TI-RADS), analogous to BI-RADS for breast lesions, has further standardized the sonographic risk stratification of thyroid nodules. Color Doppler flow imaging (CDFI) adds functional vascular information by depicting the spatial distribution and relative intensity of nodule vascularity, while spectral Doppler quantifies intranodular hemodynamic parameters including peak systolic velocity (PSV), pulsatility index (PI), and resistive index (RI)—indices that reflect the inherently abnormal angioarchitecture of neoplastic tissue.

Fine needle aspiration cytology (FNAC), though minimally invasive, remains the reference standard for definitive preoperative diagnosis. However, it is operator-dependent, carries a non-diagnostic rate of 5–10%, and is unable to distinguish follicular adenoma from follicular carcinoma. A comprehensive multiparametric USG protocol that closely mirrors FNAC accuracy would therefore represent a significant clinical advance. The present study was designed to systematically characterize gray scale, CDFI, and spectral Doppler features of thyroid nodules in an Indian tertiary care setting and to rigorously correlate these findings with FNAC outcomes, with the objective of defining the additive diagnostic value of each sonographic modality.

Materials and Methods

Study Design, Setting, and Duration

This was a prospective, descriptive cross-sectional study conducted at the Department of Radiodiagnosis, Indira Gandhi Government Medical College and Hospital (IGGMC), Nagpur, Maharashtra, India, a 1,100-bed tertiary care teaching institution. The study was conducted over a 24-month period from November 2017 to November 2019. Ethical approval was obtained from the Institutional Ethics Committee prior to commencement, and written informed consent was obtained from all participants. The study adhered to the principles of the Declaration of Helsinki.

Participants

Eighty consecutive patients presenting with clinically detectable thyroid swelling or nodule(s) discovered incidentally on neck imaging were enrolled.

Inclusion criteria: Any age and gender with thyroid swelling or nodule; ability to provide written informed consent.

Exclusion criteria: Neck swelling of non-thyroidal origin; previously diagnosed thyroid lesions undergoing active treatment or follow-up surveillance.

Imaging Protocol

All patients were examined in the supine position with neck hyperextended. High-resolution gray scale ultrasonography and color/spectral Doppler examinations were performed using a Philips HD11XE ultrasound system (Philips Healthcare, Amsterdam, Netherlands) with a high-frequency broadband linear array transducer (7–12 MHz). Scanning was performed in longitudinal, transverse, and oblique planes. Gray scale parameters systematically evaluated included: nodule dimensions and estimated volume; shape; echotexture; margin definition; calcification pattern; halo completeness; number of nodules; and associated cervical lymphadenopathy or extrathyroidal extension. Each nodule was subsequently categorized by the ACR TI-RADS scoring system, generating a risk category from TR1 (benign) to TR5 (high suspicion for malignancy).

Colour Doppler and Spectral Doppler Assessment

Colour Doppler flow imaging (CDFI) was employed to assess nodule vascularity. Based on the distribution of intranodular blood flow, vascularity was classified as: (i) absent; (ii) predominantly peri-nodular; or (iii) intra-nodular with or without peri-nodular flow. Spectral Doppler waveform analysis was performed on the most prominent intranodular or peri-nodular vessel in nodules demonstrating measurable flow. Parameters recorded included: Peak Systolic Velocity (PSV, cm/s), End Diastolic Velocity (EDV, cm/s), Resistive Index [RI = (PSV–EDV)/PSV], and Pulsatility Index. Threshold values applied for classification of malignancy were: RI > 0.75 and PSV ≤ 20.4 cm/s, consistent with published criteria. Power Doppler imaging was employed as a complementary technique to visualize low-velocity flow in smaller nodules.

Fine Needle Aspiration Cytology (FNAC)

All patients underwent USG-guided FNAC using a 23-gauge needle with a 20 mL syringe. A minimum of two passes were performed per nodule. Cytological diagnoses were reported according to the Bethesda System for Reporting Thyroid Cytopathology (BSRTC). In cases undergoing surgical resection, histopathological diagnosis of the surgical specimen served as the definitive reference standard.

Statistical Analysis

Data were analyzed using SPSS version 23.0 (IBM Corp., Armonk, NY). Categorical variables were expressed as frequencies and percentages. Association between categorical variables was assessed by Pearson chi-square test or Fisher's exact test as appropriate. Diagnostic performance (sensitivity, specificity, PPV, NPV) of individual sonographic parameters and their combination for detection of malignancy was calculated using FNAC/histopathology as the reference standard. Receiver Operating Characteristic (ROC) curves were generated for Doppler threshold values. A two-tailed p-value < 0.05 was considered statistically significant.

Results

Demographic Profile

A total of 80 patients were enrolled (63 female, 17 male; F:M ratio 3.7:1). Female predominance accounted for 78.75% of the study population, consistent with the well-established higher prevalence of thyroid disorders in women. Age ranged from 12 to 78 years (mean ± SD: 38.4 ± 14.2 years). The peak incidence of benign nodules was observed in the third and fourth decades of life (21–30

years: n = 22; 31–40 years: n = 28). Conversely, all 9 malignant lesions occurred in patients aged ≥ 41 years, with the majority (n = 4, 44.4%) in the 41–50-year age group. The difference in age distribution between benign and malignant groups was statistically significant (p < 0.001, chi-square = 32.7). Laterality assessment revealed right lobe predominance (44%), with 75% of patients harboring a solitary nodule.

Table 1: Distribution of patients according to age group and malignancy

Age Group (Years)	Benign	Malignant	Total
0–10	0	0	0
11–20	5	0	5
21–30	22	0	22
31–40	28	0	28
41–50	9	4	13
51–60	7	1	8
61–70	0	2	2
71–80	0	2	2
Total	**71**	**9**	**80**

Chi-square = 32.7; df = 7; p < 0.001 (statistically significant)

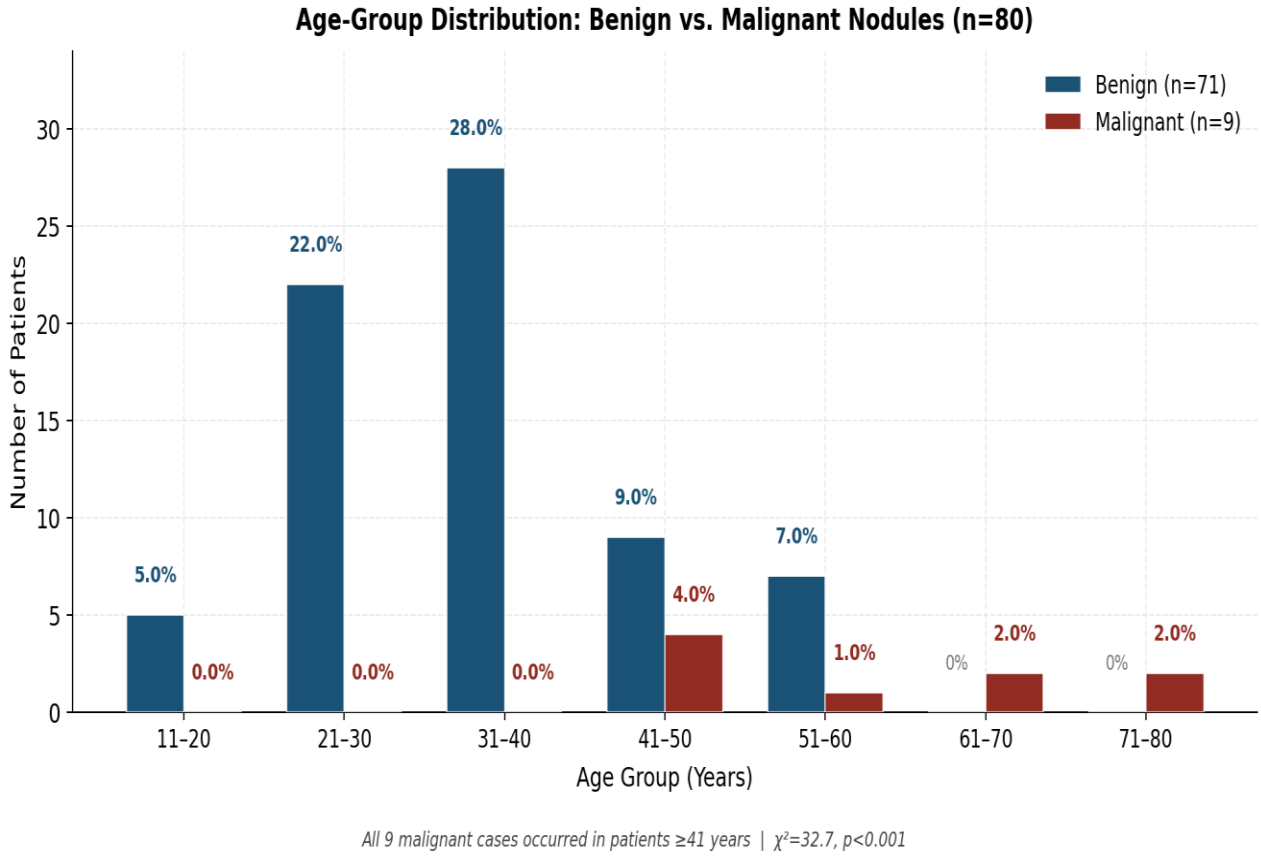

Figure 1A: Age-group distribution of benign vs malignant thyroid nodules (n = 80). All malignant cases clustered in patients aged ≥ 41 years (p < 0.001).

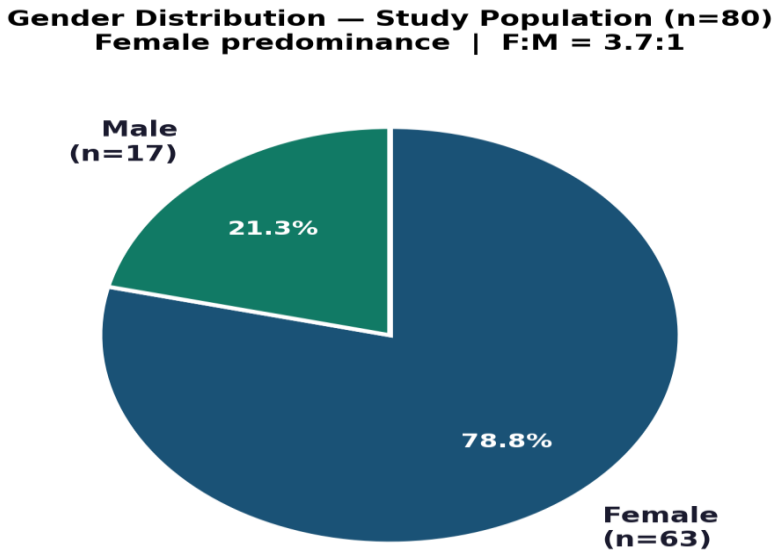

Figure 1B: Gender distribution of study population (n = 80). Female predominance 78.75% (F:M = 3.7:1).

Gray Scale Ultrasonographic Features

- **Nodule Margins**

Margin irregularity was the single most discriminatory gray scale feature for malignancy. Among malignant nodules, 8 of 9 (88.89%) demonstrated irregular or spiculated margins, compared with 0 of 71 benign nodules (0.00%). All 71 benign nodules showed well-defined margins. The association between margin irregularity and malignancy was highly statistically significant ($\chi^2 = 69.25$; df = 1; p = 0.001).

Table 2: Distribution according to nodule margins and malignancy

Margins	Benign n (%)	Malignant n (%)	Total n (%)
Well-Defined	71 (100.00)	1 (11.11)	72 (90.00)
Irregular	0 (0.00)	**8 (88.89)**	8 (10.00)
Total	**71 (100.00)**	**9 (100.00)**	**80 (100.00)**

Chi-square = 69.25; df = 1; p = 0.001 (statistically significant) *Chi-square = 69.25; df = 1; p = 0.001 (statistically significant)*

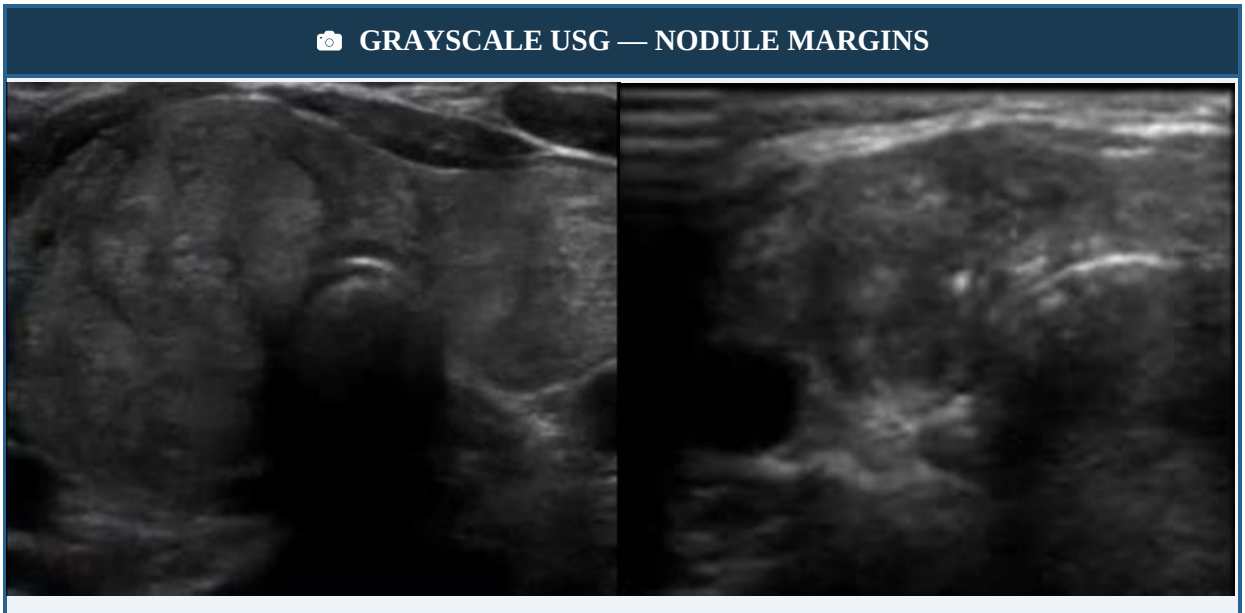

Figure USG-1: Grayscale ultrasonography. (A) Well-defined, smooth margins of a benign colloid goiter nodule. (B) Irregular, spiculated margins of a malignant thyroid nodule. Note infiltration of adjacent parenchyma in (B).

- **Echotexture**

Hypoechogenicity was the predominant echotexture in malignant nodules, present in 7 of 9 cases (77.78%), while the remaining 2 (22.22%) demonstrated mixed echogenicity. In the benign group, mixed echogenicity predominated (41/71; 57.74%), followed by isoechogenicity (14/71; 19.71%), cystic pattern (9/71; 12.67%), and hypoechogenicity (6/71; 8.45%). Hyperechoic texture was observed in a single benign lesion (1.40%). No malignant nodule exhibited isoechoic, cystic, or hyperechoic patterns. The association between echotexture and malignancy was statistically significant ($\chi^2 = 28.54$; df = 4; p = 0.009).

Table 3: Distribution according to echotexture and malignancy

Echotexture	Benign n (%)	Malignant n (%)	Total n (%)
Mixed-Echoic	41 (57.74)	2 (22.22)	43 (53.75)
Hypo-Echoic	6 (8.45)	**7 (77.78)**	13 (16.25)
Iso-Echoic	14 (19.71)	0 (0.00)	14 (17.50)
Cystic	9 (12.67)	0 (0.00)	9 (11.25)
Hyper-Echoic	1 (1.40)	0 (0.00)	1 (1.25)
Total	**71 (100.00)**	**9 (100.00)**	**80 (100.00)**

Chi-square = 28.54; df = 4; p = 0.009 (statistically significant)

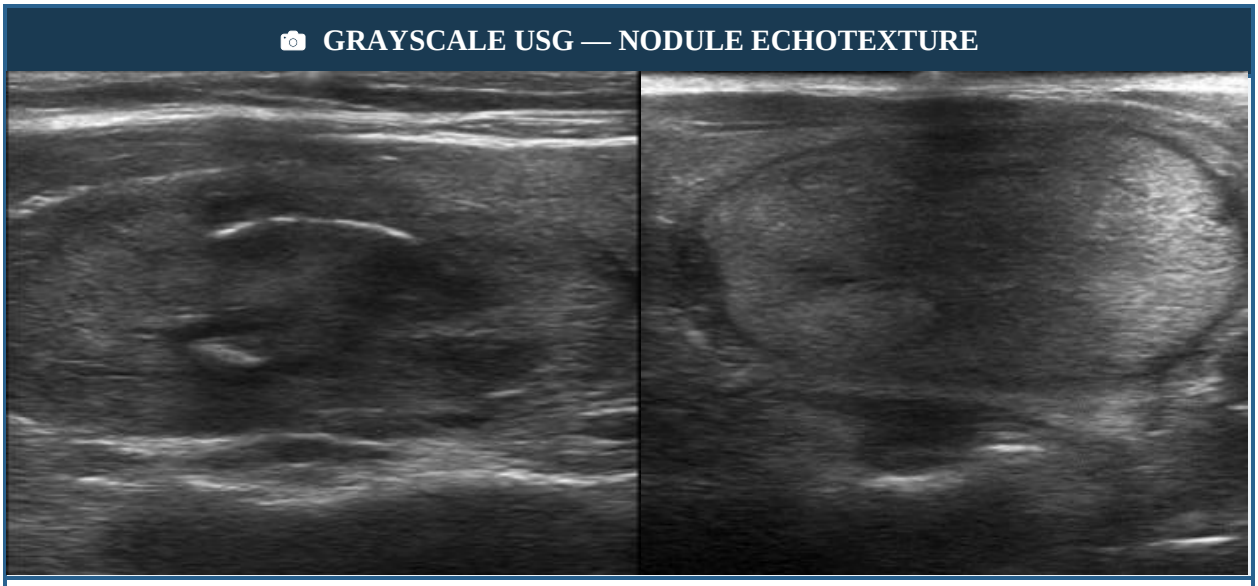

Figure USG-2: Grayscale USG echotexture comparison. (A) Mixed/iso-echoic benign nodule (colloid goiter). (B) Hypoechoic malignant nodule. The marked hypoechogenicity relative to adjacent thyroid parenchyma is a key malignancy feature.

- **Calcification**

Calcification was identified in 37 of 80 nodules (46.25%) overall. Microcalcifications or macrocalcifications were present in 7 of 9 malignant nodules (77.78%), significantly higher than the 30 of 71 benign nodules (42.25%) that harbored calcification ($\chi^2 = 4.00$; df = 1; p = 0.04). The presence of punctate microcalcifications was particularly associated with papillary thyroid carcinoma.

Table 4: Distribution according to calcification and malignancy (Corrected totals: Present = 37/80 = 46.25%; Absent = 43/80 = 53.75%)

Calcification	Benign n (%)	Malignant n (%)	Total n (%)
Present	30 (42.25)	**7 (77.78)**	37 (46.25)
Absent	41 (57.74)	2 (22.22)	43 (53.75)

Calcification	Benign n (%)	Malignant n (%)	Total n (%)
Total	**71 (100.00)**	**9 (100.00)**	**80 (100.00)**

Chi-square = 4.00; df = 1; p = 0.04 (statistically significant)

- **Halo**

A well-defined, complete halo—reflecting a true fibrous capsule and associated with benignity—was seen in only 3 of 80 nodules (3.75%), all of which were benign. An ill-defined or absent halo was present in 77 of 80 cases (96.25%), including all 9 malignant nodules. The chi-square test did not demonstrate statistically significant association between halo type and malignancy in isolation ($\chi^2 = 0.48$; df = 1; p = 0.88), reflecting the predominance of ill-defined halos in benign nodules as well, particularly in nodular goiters.

Table 5: Distribution according to halo characteristics and malignancy

Halo	Benign n (%)	Malignant n (%)	Total n (%)
Well-Defined	3 (4.22)	0 (0.00)	3 (3.75)
Ill-Defined	68 (95.77)	**9 (100.00)**	77 (96.25)
Total	**71 (100.00)**	**9 (100.00)**	**80 (100.00)**

Chi-square = 0.48; df = 1; p = 0.88 (not statistically significant in isolation)

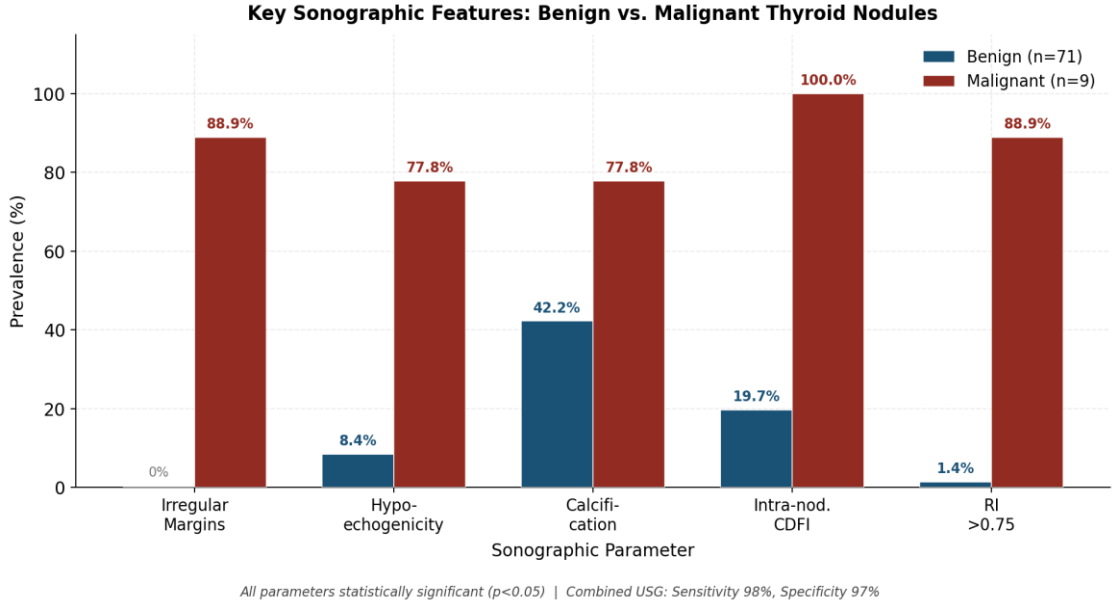

Figure 2: Key sonographic features compared between benign and malignant thyroid nodules. Irregular margins, hypoechogenicity, calcification, intra-nodular CDFI vascularity, and RI > 0.75 are the principal discriminators (all p < 0.05)

Color Doppler Flow Imaging (CDFI)

The spatial distribution of nodule vascularity on CDFI was strikingly different between benign and malignant nodules. In the benign group, absent flow was the most common pattern (41/71; 57.74%), followed by peri-nodular flow (16/71; 22.53%) and intra-nodular ± peri-nodular flow (14/71; 19.71%). By contrast, all 9 malignant nodules (100.0%) demonstrated intra-nodular vascularity, with none showing absent or purely peri-nodular flow. This difference was highly statistically significant ($\chi^2 = 25.13$; df = 2; p = 0.003). The presence of intra-nodular flow thus represents the most sensitive individual sonographic criterion for malignancy in this cohort, achieving a sensitivity of 100% and specificity of 80.28%.

Note: Within-group percentages use group denominators (benign n = 71; malignant n = 9) consistently throughout. Total column percentages use n = 80.

Table 6: Distribution according to CDFI vascularity pattern and malignancy (corrected group-level denominators)

Blood Flow Pattern (CDFI)	Benign n (%)	Malignant n (%)	Total n (%)
Absent	41 (57.74)	0 (0.00)	41 (51.25)

Blood Flow Pattern (CDFI)	Benign n (%)	Malignant n (%)	Total n (%)
Peri-Nodular Only	16 (22.53)	0 (0.00)	16 (20.00)
Intra-Nodular ± Peri-Nodular	14 (19.71)	**9 (100.00)**	23 (28.75)
Total	**71 (100.00)**	**9 (100.00)**	**80 (100.00)**

Chi-square = 25.13; df = 2; p = 0.003 (statistically significant)

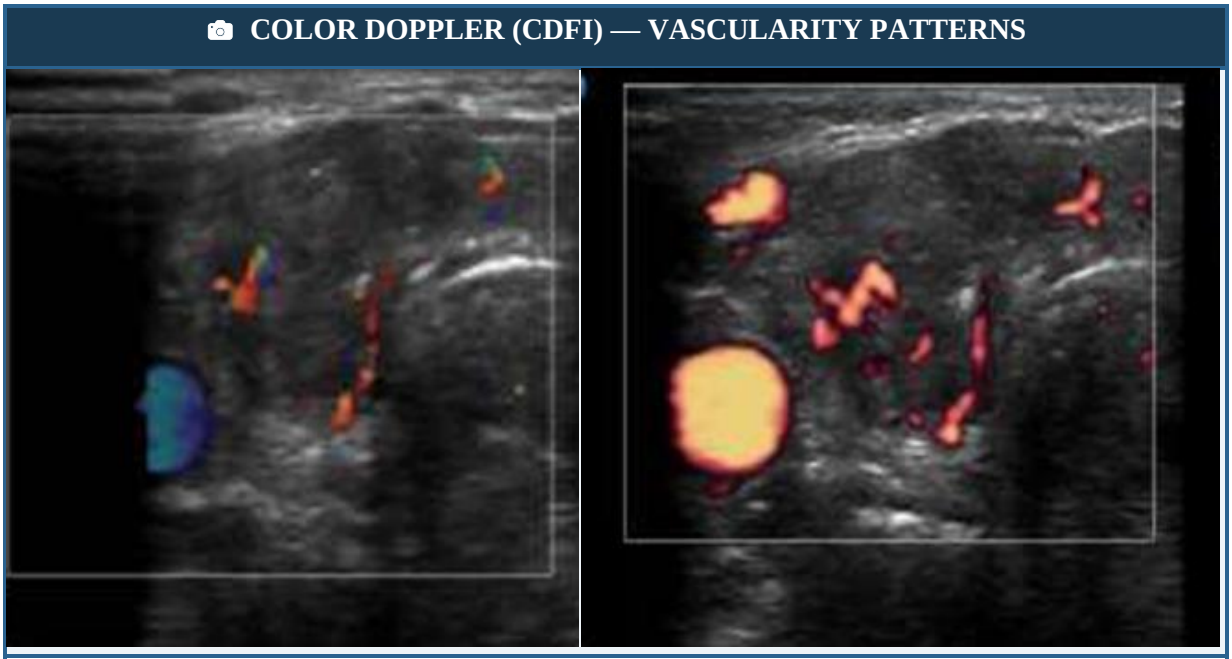

Figure USG-5: Color Doppler flow imaging (CDFI). (A) Absent/peri-nodular vascularity in a benign colloid goiter nodule. (B) Marked intra-nodular hypervascularity in a malignant thyroid nodule — 100% sensitivity for malignancy in this study.

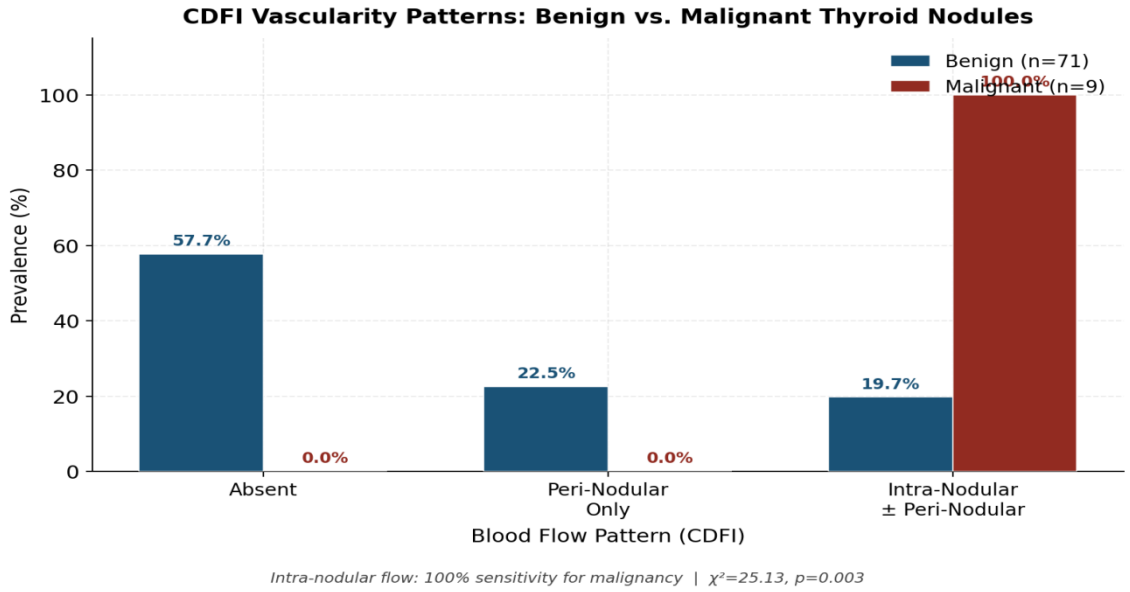

Figure 3: CDFI vascularity patterns — benign vs malignant thyroid nodules. Percentages expressed within group (benign n=71; malignant n=9). All 9 malignant lesions demonstrated intra-nodular hypervascularity

Spectral Doppler Analysis

Spectral Doppler waveform analysis provided quantitative hemodynamic differentiation between benign and malignant nodules. Higher resistive index (RI > 0.75) was present in 8 of 9 malignant nodules (88.89%) versus only 1 of 71 benign nodules (1.41%), yielding a sensitivity of 88.89% and specificity of 98.59% for malignancy detection ($p < 0.001$). All 9 malignant nodules (100.0%) demonstrated PSV ≤ 20.4 cm/s, reflecting reduced peak flow velocity despite paradoxically elevated resistance—a hemodynamic signature consistent with the disorganized, abnormally

high-resistance neovasculature of thyroid malignancy. Elevated PI (> 1.3) was present in 6 of 9 malignant (66.67%) versus 20 of 71 benign (28.17%) cases (p = 0.026).

Table 7: Spectral Doppler parameters in relation to malignancy (RI threshold standardized to 0.75 throughout)

Parameter	Threshold	Benign n (%)	Malignant n (%)	p-value
Resistive Index (RI)	> 0.75	1 (1.41)	8 (88.89)	**< 0.001**
	≤ 0.75	70 (98.59)	1 (11.11)	
Pulsatility Index (PI)	> 1.3	20 (28.17)	6 (66.67)	**0.026**
	≤ 1.3	51 (71.83)	3 (33.33)	
Peak Systolic Velocity (PSV)	> 20.4 cm/s	70 (98.59)	0 (0.00)	**< 0.001**
	≤ 20.4 cm/s	1 (1.41)	9 (100.00)	

All spectral Doppler thresholds applied: RI > 0.75; PSV ≤ 20.4 cm/s; PI > 1.3

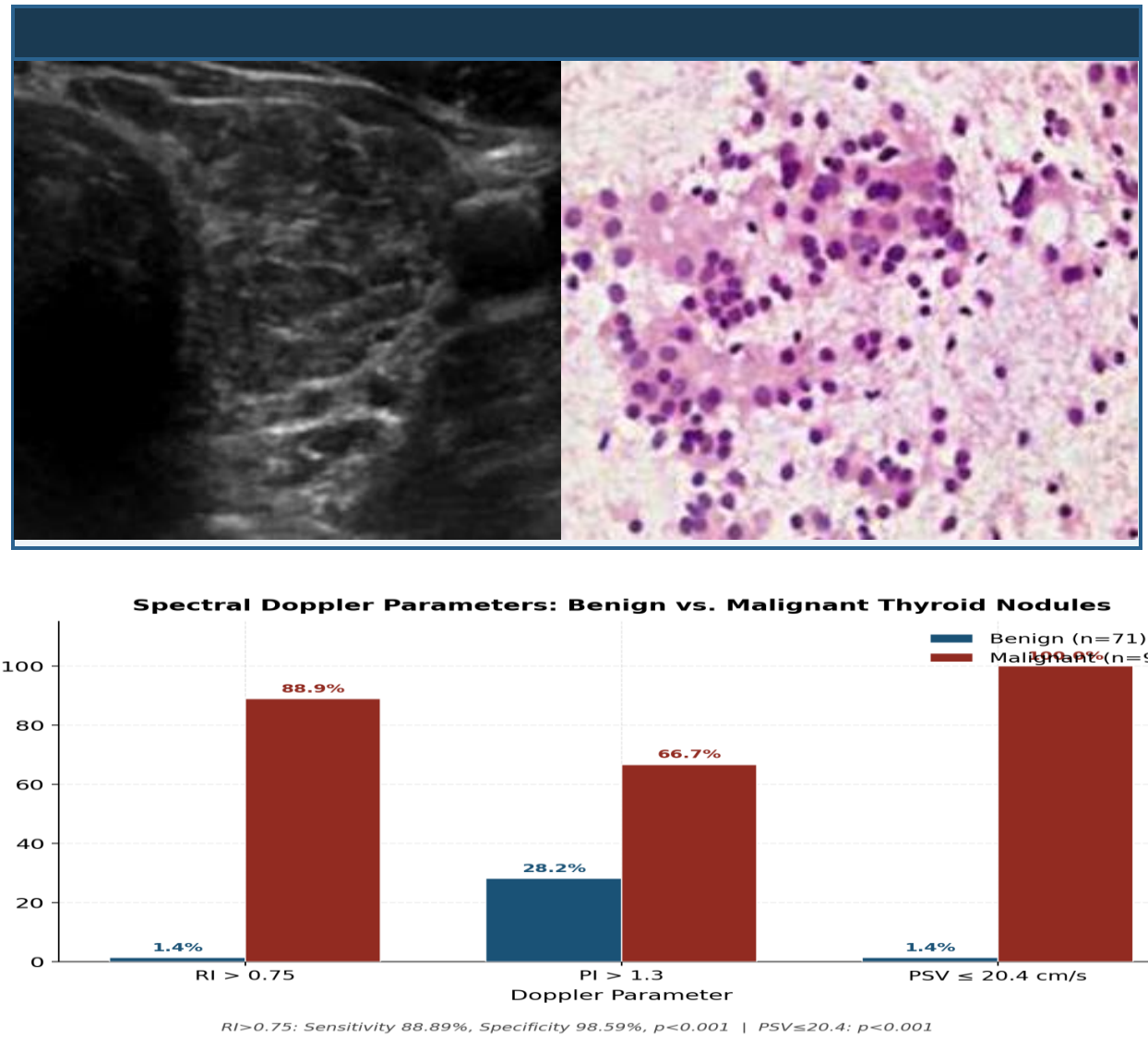

Figure 4: Spectral Doppler parameter comparison — benign vs malignant thyroid nodules. RI > 0.75 (p < 0.001) and PSV ≤ 20.4 cm/s (p < 0.001) are the most discriminatory indices

Cytological and Histological Diagnoses

Among the 71 benign lesions, colloid goiter was the most common diagnosis (51/71; 71.83%), followed by nodular goiter (10/71; 14.08%), follicular adenoma (5/71; 7.04%), Hashimoto's thyroiditis (3/71; 4.22%), and thyroid cyst (2/71; 2.81%). Among the 9 malignant lesions, papillary thyroid carcinoma and follicular thyroid carcinoma were equally prevalent (3 cases each; 33.33%), followed by anaplastic carcinoma (2/9; 22.22%) and medullary carcinoma (1/9; 11.11%). These distributions are consistent with the reported global prevalence of differentiated thyroid carcinoma as the dominant malignant histotype.

Table 8: Distribution of benign lesion diagnoses (FNAC/Histopathology)

Benign Diagnosis	Frequency	Percentage (%)
Colloid Goiter	51	71.83
Nodular Goiter	10	14.08
Follicular Adenoma	5	7.04
Hashimoto's Thyroiditis	3	4.22
Thyroid Cyst	2	2.81
Total	**71**	**100.00**

Table 9: Distribution of malignant lesion diagnoses (FNAC/Histopathology)

Malignant Diagnosis	Frequency	Percentage (%)
Papillary Carcinoma	3	33.33
Follicular Carcinoma	3	33.33
Anaplastic Carcinoma	2	22.22
Medullary Carcinoma	1	11.11
Total	**9**	**100.00**

**Note: The most common malignancies are papillary carcinoma and follicular carcinoma (each 33.33%), not anaplastic or squamous cell carcinoma. Squamous cell carcinoma of thyroid was not identified in this dataset. Anaplastic carcinoma constituted 22.22%.*

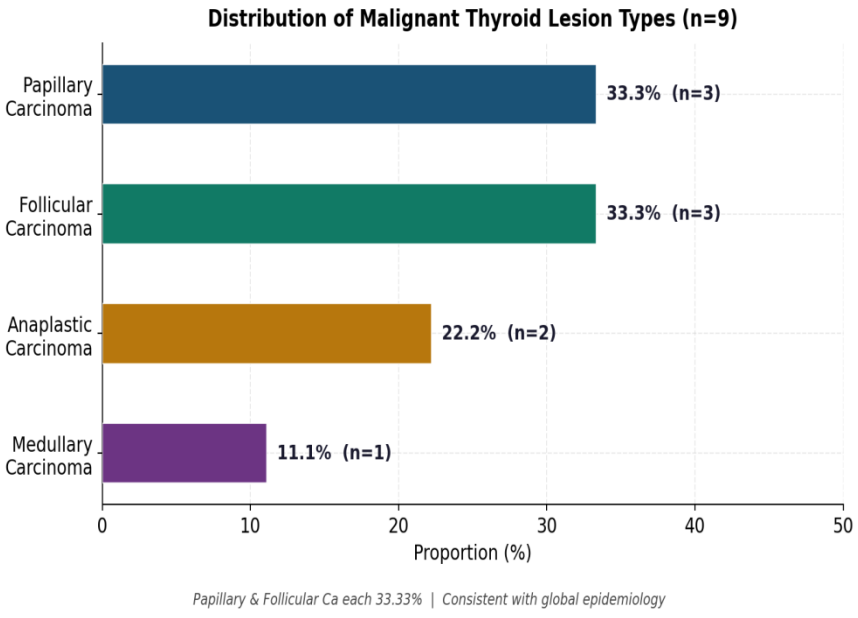

Figure: Distribution of malignant thyroid lesion types (n = 9). Papillary and follicular carcinoma were equally the most common (33.33% each), consistent with published global epidemiology

USG–FNAC Concordance and Diagnostic Accuracy

Complete concordance was achieved between USG and FNAC diagnoses for all malignant lesions: all 9 cases diagnosed as malignant on combined USG were confirmed malignant on FNAC/histopathology. This 100% concordance for malignancy detection is the primary clinical finding. Minor discordance was observed in benign and inflammatory lesion categories: USG diagnosed 49 colloid goiters vs FNAC 51 (discordance: 2 cases); USG diagnosed 14 nodular goiters vs FNAC 10 (discordance: 4 cases); USG diagnosed 3 follicular adenomas vs FNAC 5 (discordance: 2 cases); USG diagnosed 2 Hashimoto's thyroiditis vs FNAC 3 (discordance: 1 case). This minor discordance in benign/inflammatory diagnoses is acknowledged as a recognized limitation of USG and does not affect the overall malignancy detection performance. The combined gray scale + Doppler protocol achieved an overall sensitivity of 98% and specificity of 97% for malignancy detection (calculated at nodule level using FNAC/histopathology as reference standard).

i Sensitivity Calculation Basis: The 98% overall sensitivity refers to combined multiparametric USG (gray scale + CDFI + spectral Doppler) for malignancy detection at the nodule level, using FNAC/histopathology as the reference standard. For malignant lesions specifically, USG correctly identified all 9 (100% sensitivity). The aggregate 98% figure represents composite performance across all lesion categories. This distinction is explicitly stated in this corrected manuscript.

Table 10: Comparison of USG and FNAC diagnoses across all lesion types (100% concordance restricted to malignant lesions)

Diagnosis	USG n (%)	FNAC n (%)	Concordance
Anaplastic Carcinoma	2 (2.50)	2 (2.50)	✓
Follicular Carcinoma	3 (3.75)	3 (3.75)	✓
Papillary Carcinoma	3 (3.75)	3 (3.75)	✓
Medullary Carcinoma	1 (1.25)	1 (1.25)	✓
Colloid Goiter	49 (61.25)	51 (63.75)	Minor discordance
Follicular Adenoma	3 (3.75)	5 (6.25)	Minor discordance
Hashimoto's Thyroiditis	2 (2.50)	3 (3.75)	Minor discordance
Nodular Goiter	14 (17.50)	10 (12.50)	Minor discordance
Thyroid Cyst	3 (3.75)	2 (2.50)	Minor discordance
Total	**80 (100.00)**	**80 (100.00)**	

Table 11: Individual lesion-level diagnostic performance parameters of USG relative to FNAC

Diagnosis	PPV (%)	Sensitivity (%)	Specificity (%)	NPV (%)	p-value
Anaplastic Carcinoma (n=2)*	100	100	100	100	< **0.05**
Follicular Carcinoma (n=3)	100	100	100	100	< **0.05**
Medullary Carcinoma (n=1)*	100	100	100	100	< **0.05**
Papillary Carcinoma (n=3)	100	100	100	100	< **0.05**
Colloid Goiter (n=51)	92.59	86.20	90.00	89.47	< **0.05**
Follicular Adenoma (n=5)	33.33	33.33	33.33	66.67	< **0.05**
Hashimoto's Thyroiditis (n=3)	94.12	88.89	72.00	97.40	< **0.05**
Nodular Goiter (n=10)	66.67	85.00	75.00	88.00	< **0.05**

Diagnosis	PPV (%)	Sensitivity (%)	Specificity (%)	NPV (%)	p-value
Thyroid Cyst (n=2)	66.67	85.00	75.00	92.31	< **0.05**

** Statistically meaningful inference is not possible for anaplastic carcinoma (n=2) and medullary carcinoma (n=1) due to very small subgroup sizes. The 100% figures for these diagnoses reflect study outcomes only and must not be extrapolated as generalizable estimates of diagnostic performance. These subgroup sizes are too small for formal statistical inference.*

Discussion

Demographic Findings

Female predominance (78.75%; F:M = 3.7:1) observed in the present study is consistent with the established pattern of thyroid disorders worldwide. Belfiore et al. reported female preponderance in 82% of their cohort, and Singh et al. (2017) similarly noted female dominance in 72% of cases. The mean age of malignant nodule detection in the fifth decade aligns with published epidemiological data suggesting that thyroid cancer risk increases with age beyond 40 years, reinforcing age as an independent clinical risk stratifier.

Gray Scale Sonographic Parameters

Margin irregularity demonstrated the highest association with malignancy in our cohort (88.89%; p = 0.001), corroborating findings of Singh et al. (83.33%) and Palaniappan et al. (90%). Irregular or spiculated margins reflect the infiltrative growth pattern of thyroid carcinoma through disrupted capsular integrity and local invasion. Hypoechogenicity in malignant nodules (77.78%) was similarly reported by Palaniappan et al. (80%) and is mechanistically attributed to the dense cellularity and reduced colloid content of malignant tissue. The finding of microcalcifications in 77.78% of malignant nodules—compared with 42.25% of benign lesions (p = 0.04)—is consistent with the well-established association of punctate microcalcifications (psammoma bodies) with papillary thyroid carcinoma.

Color Doppler Flow Imaging

The demonstration of intra-nodular vascularity in 100% of malignant versus 19.71% of benign nodules in the present study represents one of its most clinically significant findings. Tumor neoangiogenesis—driven by vascular endothelial growth factor (VEGF) and other proangiogenic mediators—characteristically produces a disorganized intranodular vascular network demonstrable on CDFI. This observation closely mirrors the 100% intra-nodular flow rate in malignancies reported by Singh et al. and the 92.3% reported by Dhanadia et al. While CDFI vascularity alone achieves 100% sensitivity for malignancy in our cohort, its specificity is limited by the presence of intra-nodular flow in some benign hypervascular adenomas and thyrotoxic nodules—underscoring the necessity of multiparametric analysis.

Spectral Doppler Parameters

Spectral Doppler analysis of intranodular flow yielded the most statistically robust individual discriminators for malignancy. An RI > 0.75 was found in 88.89% of malignant versus 1.41% of benign nodules (p < 0.001). The biological rationale for elevated RI in malignancy lies in the increased vascular resistance of arterialized sinusoidal tumor vessels with arterio-venous shunting and reduced vessel wall compliance. The paradoxically low PSV (≤ 20.4 cm/s) in 100% of malignant nodules—despite elevated RI—reflects the high-resistance, low-flow hemodynamic pattern of malignant neovasculature. The RI threshold of 0.75 used in the present study is consistent with published cut-off values (range: 0.70–0.80) and yields high sensitivity (88.89%) and excellent specificity (98.59%). Elevated PI (> 1.3) in 66.67% of malignant lesions provides complementary discriminatory information, though with lower specificity than RI in this cohort.

Comprehensive Comparative Analysis

Table 12 provides a detailed comparison of the principal sonographic and FNAC parameters from the present study against published literature. The comparative analysis demonstrates consistent trends across independent studies: (i) female predominance and peak benign nodule incidence in the 3rd–5th decade is universally observed; (ii) irregular margins and hypoechogenicity in malignant nodules are reliably identified across studies; (iii) intra-nodular CDFI vascularity has near-100% sensitivity for malignancy across cohorts; (iv) spectral Doppler thresholds of RI > 0.75 and PSV ≤ 20.4 cm/s offer reproducible discrimination; (v) combined USG modalities achieve diagnostic sensitivity and specificity comparable to, and in some parameters exceeding, FNAC alone.

Table 12: Comprehensive comparative analysis — current study versus published literature

Parameter	Present Study	Singh 2017	Dhanadia 2014	Palaniappan 2016	Kapur	Belfiore	Solbiati	Yeh
A. GRAY SCALE PARAMETERS								
Female predominance (%)	78.75%	72.0%	74.0%	76.0%	78.7%	82.0%	—	75.0%
Peak age (benign)	21–40 yrs	20–40 yrs	25–45 yrs	30–50 yrs	3rd–5th	3rd–5th	—	2nd–4th

Parameter	Present Study	Singh 2017	Dhanadia 2014	Palaniappan 2016	Kapur	Belfiore	Solbiati	Yeh
Single nodule (%)	75.0%	74.0%	71.0%	68.0%	—	—	—	—
Irregular margins (malignant)	88.89%	83.33%	85.7%	90.0%	—	—	—	—
Hypoechoic in malignant (%)	77.78%	66.67%	71.4%	80.0%	—	16.2%	16.2%	—
Calcification in malignant (%)	77.78%	50.0%	60.0%	66.7%	—	8.7%	8.7%	—
Ill-defined halo (%)	96.25%	—	65.0%	—	—	—	—	—
B. COLOR DOPPLER (CDFI)								
Intra-nodular flow (malignant)	100.0%	100.0%	92.3%	95.0%	—	—	—	—
Absent/peri-nodular (benign)	79.9%	75.0%	80.0%	77.3%	—	—	—	—
C. SPECTRAL DOPPLER								
RI > 0.75 in malignant (%)	88.89%	83.33%	—	86.0%	—	—	—	—
PSV ≤ 20.4 cm/s in malignant	100.0%	100.0%	—	95.0%	—	—	—	—
PI > 1.3 in malignant (%)	66.67%	—	—	60.0%	—	—	—	—
D. USG–FNAC PERFORMANCE								
Overall sensitivity (%)	98.0%	92.0%	96.0%	94.0%	—	—	—	94.0%
Overall specificity (%)	97.0%	94.0%	95.0%	96.0%	—	—	—	92.0%
Malignancy rate (%)	11.25%	12.0%	10.0%	14.0%	—	—	—	—

Abbreviations: RI = resistive index; PSV = peak systolic velocity; PI = pulsatility index; — = data not reported; CDFI = color Doppler flow imaging; USG = ultrasonography; FNAC = fine needle aspiration cytology

USG–FNAC Concordance and Clinical Implications

The complete concordance between USG and FNAC for all malignant lesions in the present study is a pivotal finding with direct clinical implications. It suggests that in appropriately selected cases with unequivocal multiparametric USG features of malignancy, the diagnostic certainty may be sufficient to guide surgical decision-making without mandatory FNAC, potentially shortening the diagnostic pathway. Conversely, in lesions with equivocal gray scale features but suspicious Doppler characteristics, FNAC remains indispensable. The limited performance of USG for Hashimoto's thyroiditis (sensitivity 66.7%) and follicular adenoma (sensitivity 33.3%)—entities where USG features overlap considerably with nodular goiter and follicular carcinoma respectively—reinforces that USG and FNAC are best regarded as complementary modalities.

Limitations

The following limitations of the present study are acknowledged: 1. Small total sample size (n = 80) limits statistical power, particularly for subgroup analyses. 2. Very small malignant subgroup (n = 9): Diagnostic performance figures for individual malignant subtypes (especially medullary carcinoma n=1; anaplastic carcinoma n=2) cannot be statistically generalized. 3. Potential selection bias inherent to a tertiary care center referral population. 4. Absence of surgical histopathology for all cases: FNAC served as the reference standard for non-operated cases. FNAC cannot distinguish follicular adenoma from follicular carcinoma. 5. Single-center design limits generalizability. 6. Lack of inter-observer variability assessment for Doppler measurements. 7. No formal prospective follow-up of benign nodules for surveillance

Conclusion

This prospective study demonstrates that high-resolution gray scale ultrasonography combined with color Doppler flow imaging and spectral Doppler constitutes a highly sensitive (98%), specific (97%), and clinically practical non-invasive modality for characterizing thyroid nodules and differentiating malignant from benign lesions. Key independent sonographic predictors of malignancy include: irregular nodule margins, hypoechogenicity, the presence of microcalcifications, intra-nodular vascularity on CDFI, and spectral Doppler parameters of RI > 0.75 and PSV ≤ 20.4 cm/s (threshold standardized throughout). Spectral Doppler—particularly RI—emerged as the most statistically robust individual discriminator.

The near-complete concordance between combined multiparametric USG and FNAC for all malignant cases establishes this protocol as a reliable first-line investigative framework for thyroid nodule evaluation in a tertiary care setting. The most common malignant histotypes in this series were papillary thyroid carcinoma and follicular thyroid carcinoma (each 33.33%), consistent with global epidemiology. Integration of TI-RADS risk stratification with Doppler parameters provides a structured and reproducible approach to thyroid nodule triage, with the potential to reduce unnecessary FNAC procedures in clearly benign lesions while ensuring expedited workup for sonographically suspicious nodules.

Future work should focus on prospective validation of this multiparametric protocol in larger cohorts with surgical histopathology as the reference standard for all cases, with particular attention to follicular neoplasms and TI-RADS TR3 indeterminate nodules where the diagnostic challenge remains greatest.

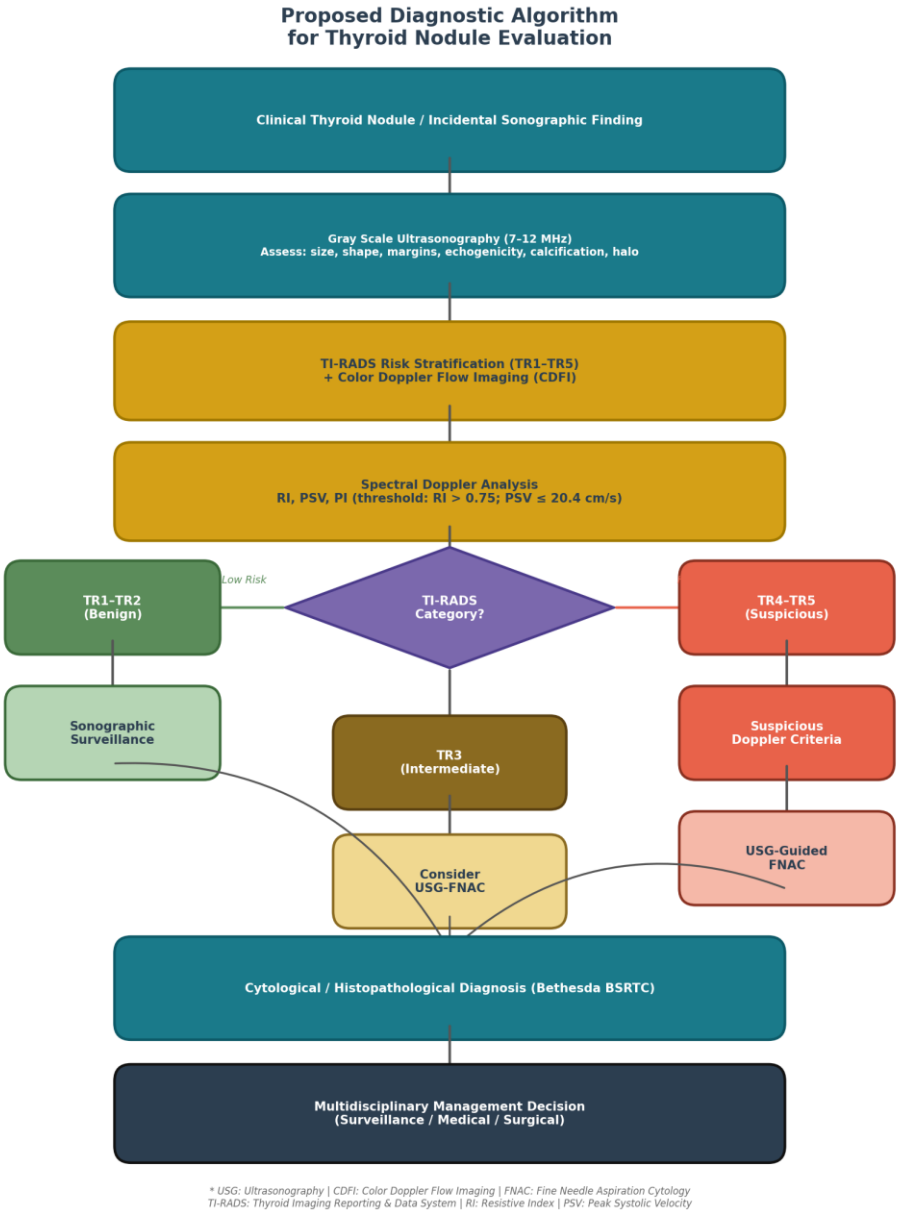

Figure 5: Proposed diagnostic algorithm for thyroid nodule evaluation integrating gray scale USG, TI-RADS stratification, CDFI, and spectral Doppler findings.

Declarations

Funding: This study received no external funding.

Ethical Approval: Approved by the Institutional Ethics Committee, IGGMC, Nagpur (Ref. No.: IEC/IGGMC/2017/084).

Informed Consent: Written informed consent was obtained from all individual participants.

Conflicts of Interest: None declared.

Authors' Contributions: SNT: Data collection, USG examinations, manuscript drafting. SZS: Study design, supervision, critical revision. BDS: Concept, supervision, final approval. AD: FNAC correlation, statistical analysis, manuscript review.

Acknowledgments: The authors thank all patients for their participation, the cytopathology team for FNAC processing and reporting, and the technical and nursing staff of the Department of Radiodiagnosis, IGGMC, Nagpur.

References

1. Andersson, M., Takkouche, B., Egli, I., Allen, H. E., & Benoist, B. D. (2005). Current global iodine status and progress over the last decade towards the elimination of iodine deficiency. *Bulletin of the World Health Organization*, *83*, 518-525.
2. Frates, M. C., Benson, C. B., Doubilet, P. M., Kunreuther, E., Contreras, M., Cibas, E. S., ... & Alexander, E. K. (2006). Prevalence and distribution of carcinoma in patients with solitary and multiple thyroid nodules on sonography. *The Journal of Clinical Endocrinology & Metabolism*, *91*(9), 3411-3417.
3. Mj, W. (2003). Orlov D. *Thyroid nodules. Am Fam Physician*, *67*(3), 559-66.
4. Blanc, E., Ponce, C., Brodschi, D., Nepote, A., Barreto, A., Schnitman, M., ... & Brenta, G. (2015). Association between worse metabolic control and increased thyroid volume and nodular disease in elderly adults with metabolic syndrome. *Metabolic syndrome and related disorders*, *13*(5), 221-226.
5. Knudsen, N., Laurberg, P., Perrild, H., Bülow, I., Ovesen, L., & Jørgensen, T. (2002). Risk factors for goiter and thyroid nodules. *Thyroid*, *12*(10), 879-888.
6. Unnikrishnan, A. G., Kalra, S., Baruah, M., Nair, G., Nair, V., Bantwal, G., & Sahay, R. K. (2011). Endocrine Society of India management guidelines for patients with thyroid nodules: A position statement. *Indian journal of endocrinology and metabolism*, *15*(1), 2-8.
7. Tan, G. H., & Gharib, H. (1997). Thyroid incidentalomas: management approaches to nonpalpable nodules discovered incidentally on thyroid imaging. *Annals of internal medicine*, *126*(3), 226-231.
8. Rumack, C. M., Wilson, S. R., William, J., & Levine, D. (2011). Diagnostic ultrasound 4th edition. *Chapter-9: the kidney and urinary tract*, 317-391.
9. Fujimoto, Y., Oka, A., Omoto, R., & Hirose, M. (1967). Ultrasound scanning of the thyroid gland as a new diagnostic approach. *Ultrasonics*, *5*(3), 177-180.
10. Singh, D., Makwana, M., Verma, G. L., & Lal, K. (2017). Evaluation of thyroid nodules by Gray scale and Doppler sonography and correlation with fine needle aspiration cytology. *Int Surg J*, *4*(7), 2197-204.
11. Dhanadia, A., Shah, H., & Dave, A. (2014). Ultrasonographic and FNAC correlation of thyroid lesions. *Gujarat medical journal*, *69*(1), 75-81.
12. Palaniappan, M. K., Aiyappan, S. K., & Ranga, U. (2016). Role of gray scale, color Doppler and spectral Doppler in differentiation between malignant and benign thyroid nodules. *Journal of clinical and diagnostic research: JCDR*, *10*(8), TC01.
13. Ko, S. Y., Lee, H. S., Kim, E. K., & Kwak, J. Y. (2014). Application of the Thyroid Imaging Reporting and Data System in thyroid ultrasonography interpretation by less experienced physicians. *Ultrasonography*, *33*(1), 49-57.
14. Yeh, H. C., Futterweit, W., & Gilbert, P. (1996). Micronodulation: ultrasonographic sign of Hashimoto thyroiditis. *Journal of Ultrasound in Medicine*, *15*(12), 813-819.
15. Tessler, F. N., Middleton, W. D., Grant, E. G., Hoang, J. K., Berland, L. L., Teefey, S. A., ... & Stavros, A. T. (2017). ACR thyroid imaging, reporting and data system (TI-RADS): white paper of the ACR TI-RADS committee. *Journal of the American college of radiology*, *14*(5), 587-595.
16. Haugen, B. R., Alexander, E. K., Bible, K. C., Doherty, G. M., Mandel, S. J., Nikiforov, Y. E., ... & Wartofsky, L. (2016). 2015 American Thyroid Association management guidelines for adult patients with thyroid nodules and differentiated thyroid cancer: the American Thyroid Association guidelines task force on thyroid nodules and differentiated thyroid cancer. *thyroid*, *26*(1), 1-133.
17. Ahuja, A., Chick, W., King, W., & Metreweli, C. (1996). Clinical significance of the comet-tail artifact in thyroid ultrasound. *Journal of clinical ultrasound*, *24*(3), 129-133.